The Journal of Neuroscience, September 15, 1999, *19*(18):7742–7756

Two Types of K^+ Channel Subunit, Erg1 and KCNQ2/3, Contribute to the M-Like Current in a Mammalian Neuronal Cell

A. A. Selyanko,[1] J. K. Hadley,[1] I. C. Wood,[2] F. C. Abogadie,[2] P. Delmas,[2] N. J. Buckley,[2] B. London,[3] and D. A. Brown[1]

[1]*Department of Pharmacology,* [2]*Wellcome Laboratory for Molecular Pharmacology, University College London, London, WC1E 6BT, United Kingdom, and* [3]*Cardiovascular Institute, University of Pittsburgh Medical Center, Pittsburgh, Pennsylvania 15213*

The potassium M current was originally identified in sympathetic ganglion cells, and analogous currents have been reported in some central neurons and also in some neural cell lines. It has recently been suggested that the M channel in sympathetic neurons comprises a heteromultimer of *KCNQ2* and *KCNQ3* (Wang et al., 1998) but it is unclear whether all other M-like currents are generated by these channels. Here we report that the M-like current previously described in NG108–15 mouse neuroblastoma x rat glioma cells has two components, "fast" and "slow", that may be differentiated kinetically and pharmacologically. We provide evidence from PCR analysis and expression studies to indicate that these two components are mediated by two distinct molecular species of K^+ channel: the fast component resembles that in sympathetic ganglia and is probably carried by *KCNQ2/3* channels, whereas the slow component appears to be carried by merg1a channels. Thus, the channels generating M-like currents in different cells may be heterogeneous in molecular composition.

Key words: potassium channels; neuroblastoma x glioma hybrid cells; M current; sympathetic neuron; Erg1; KCNQ

The M current ($I_{K(M)}$) is a low-threshold, slowly activating potassium current that exerts an inhibitory control over neuronal excitability; this inhibition can be relieved by neurotransmitters acting on G-protein-coupled receptors, leading to enhanced excitability and reduced spike-frequency adaptation (Brown, 1988; Marrion, 1997). The current was originally described in sympathetic neurons (Brown and Adams, 1980; Constanti and Brown, 1981), and analogous currents have subsequently been identified in a variety of other neuronal and non-neuronal cells. Because the precise kinetic and pharmacological properties of the current vary somewhat in different cell types, the name "M-like" is often applied to this current family.

Recently, evidence has been provided to indicate that the channels that generate the M current in rat sympathetic neurons are composed of a heteromeric assembly of *KCNQ2* and *KCNQ3* subunits (Wang et al., 1998; see also Yang et al., 1998). These are two homologs of the *KCNQ1* (*KvLQT1*) channel, mutations of which are responsible for one form of the cardiac "long QT" syndrome (Yang et al., 1997). In contrast, *KCNQ2* and *KCNQ3* are restricted to the nervous system, and mutations in these channels are associated with a form of infant epilepsy termed "benign familial neonatal convulsions" (Biervert et al., 1998; Charlier et al., 1998; Schroeder et al., 1998; Singh et al., 1998). However, it is not yet known whether all M-like channels are composed of these two subunits (or homologs thereof), or whether members of other K^+ channel gene families might contribute to the generation of M-like currents.

In the present experiments, we have attempted to identify the molecular species of K^+ channels that generate the M-like current ($I_{K(M,ng)}$) in NG108–15 mouse neuroblastoma x rat glioma cells. These currents have been particularly well characterized (Higashida and Brown, 1986; Brown and Higashida, 1988a,b; Fukuda et al., 1988; Schafer et al., 1991; Robbins et al., 1992, 1993; Selyanko et al., 1995). Like the channels in sympathetic neurons, they are inhibited by transmitters acting on G-protein-linked receptors coupled to phospholipase C (e.g., bradykinin and M_1 and M_3 muscarinic receptors) (Higashida and Brown, 1986; Fukuda et al., 1988), with similar consequences for cell firing (Robbins et al., 1993). On the other hand, the kinetics of $I_{K(M,ng)}$ appear more complex than those of the ganglionic M current (Robbins et al., 1992), and the two currents differ in their sensitivities to 9-aminotetrahydroacridine (cf. Marsh et al., 1990; Robbins et al., 1992) and linopirdine (cf. Aiken et al., 1995; Lamas et al., 1997; Noda et al., 1998). It has previously been suggested that *Shaker*-type Kv1.2 channels, cloned from NG108–15 cells (Yokoyama et al., 1989), may contribute to $I_{K(M,ng)}$ (Morielli and Peralta, 1995). However, the insensitivity of $I_{K(M,ng)}$ to dendrotoxin (Selyanko et al., 1995) makes this unlikely. Instead, we provide evidence to indicate that two different types of K^+ channel contribute to the M-like current in NG108–15 cells: the mouse *ether-a-go-go*-related gene (merg1a), also expressed in the brain (London et al., 1997), and *KCNQ2*/*KCNQ3*, the proposed substrate for the ganglionic current (Wang et al., 1998).

MATERIALS AND METHODS

Cell cultures. NG108–15 mouse neuroblastoma x rat glioma hybrid cells, subclone BM8 (PM1), transfected to express pig brain M_1 muscarinic receptor (Fukuda et al., 1988), were cultured and differentiated as described previously (Robbins et al., 1992). Chinese hamster ovary (CHO) cells stably transfected with cDNA encoding human M_1 muscarinic

Received May 18, 1999; revised June 28, 1999; accepted July 2, 1999.

B.L. was supported by a Grant-In-Aid from the American Heart Association, and the other authors were supported by the United Kingdom Medical Research Council and the Wellcome Trust. We thank Misbah Malik-Hall, Brenda Browning, and Mariza Dayrell for tissue culture and Svjetlana Miocinovic (Biology Program, CalTech, Pasadena, CA) for participation in some experiments.

Correspondence should be addressed to Dr. A. A. Selyanko, Department of Pharmacology, University College London, Gower Street, London WC1E 6BT, UK.

Copyright © 1999 Society for Neuroscience 0270-6474/99/197742-15$05.00/0

Table 1. Fast and slow kinetic components of $I_{K(M,ng)}$ and their comparison with the kinetics of $I_{K(M)}$ and I_{Merg1}

	τ, contribution		
Current	Fast	Slow	
$I_{K(M,ng)}$			
Total (control)	117 ± 5 msec	658 ± 29 msec	3434 ± 159 msec
	33.1 ± 2.1% (86/101)	25.7 ± 1.7% (82/101)	41.2 ± 2.2% (86/101)
		333 ± 126 msec	2356 ± 247 msec
		42.5 ± 5.1% (14/101)	57.6 ± 5.1% (15/101)
Fast (WAY-insensitive)	104 ± 7 msec (37)		
Slow (WAY-sensitive)		456 ± 29 msec	2718 ± 156 msec
		41.7 ± 3.5% (34/36)	58.3 ± 3.5% (36/36)
$I_{K(M)}$	93 ± 5.6 msec (n = 15)		
I_{merg1a}		183 ± 10.6 msec	1012 ± 85 msec
		64.6 ± 2.4% (22/23)	35.4 ± 2.4% (23/23)
I_{merg1b}		37.1 ± 19.4 msec	112 ± 42.5 msec
		70.8 ± 15.8% (3/3)	29.2 ± 15.8% (3/3)

$I_{K(M,ng)}$, $I_{K(M)}$, I_{merg1a}, and I_{merg1b} were recorded from NG108-15, mouse sympathetic, and CHO cells, respectively. Deactivation was recorded in response to a voltage step to −50 mV from a holding potential of −20 mV ($I_{K(M,ng)}$ and $I_{K(M)}$) or 0 mV (I_{merg1a} and I_{merg1b}). Means ± SEM of τ and contributions were obtained from deactivation relaxations recorded at −50 mV. Number of cells in parentheses; see Results.

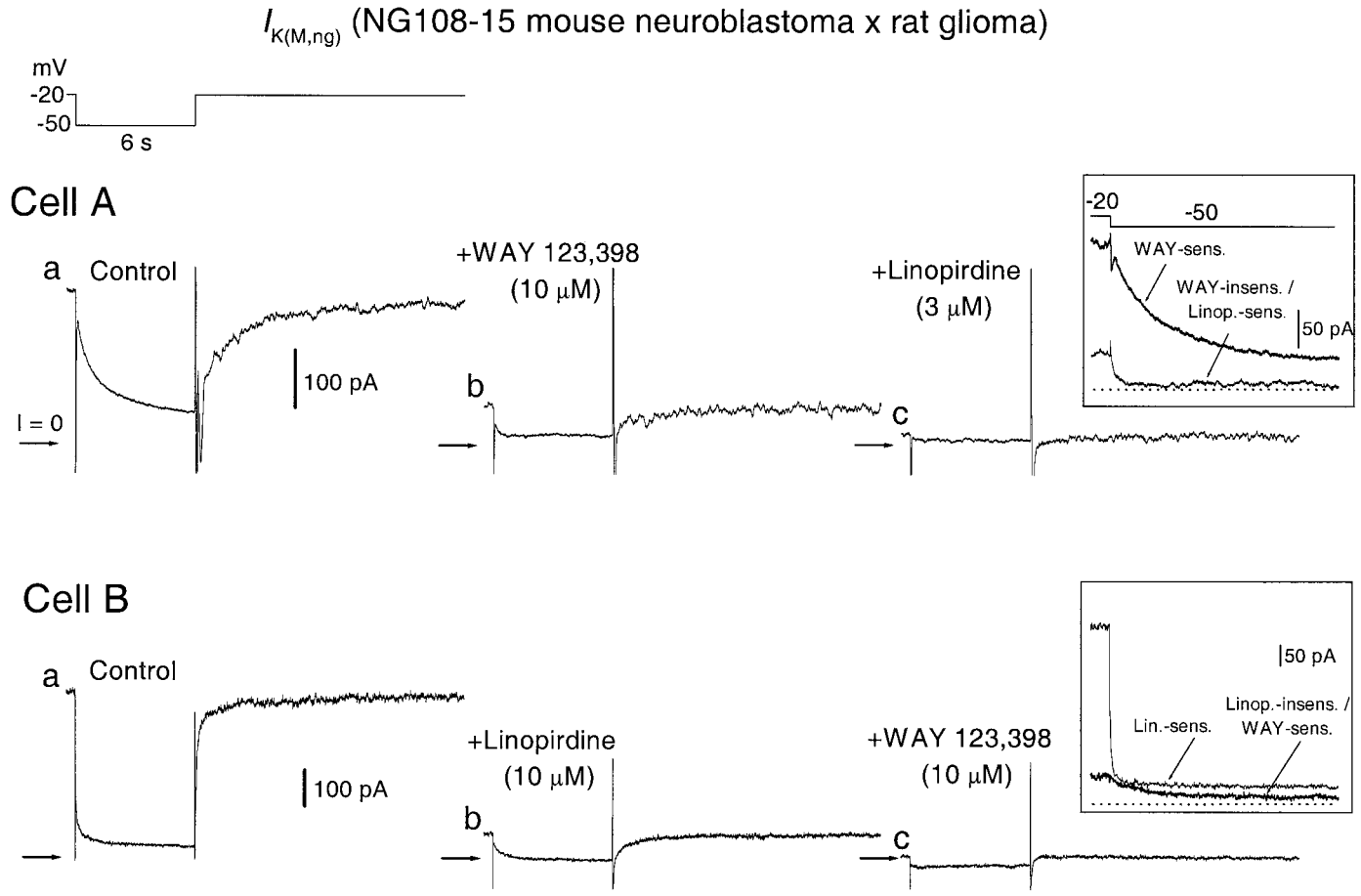

Figure 1. Pharmacological separation of two components of the M-like ($I_{K(M,ng)}$) current in NG108–15 mouse neuroblastoma x rat glioma cells. M-like currents recorded in two cells (*A, B*) as deactivating tail currents produced by voltage steps from −20 mV (holding potential) to −50 mV. In each cell, the control current had two different components, fast and slow, which could be blocked by WAY 123,398 and linopirdine, respectively. *Insets* on the *right* show the difference (blocker-sensitive) currents. The current in *A* consisted predominantly of the slow component (blocked by WAY 123,398), whereas that in *B* was predominantly fast and blocked by linopirdine.

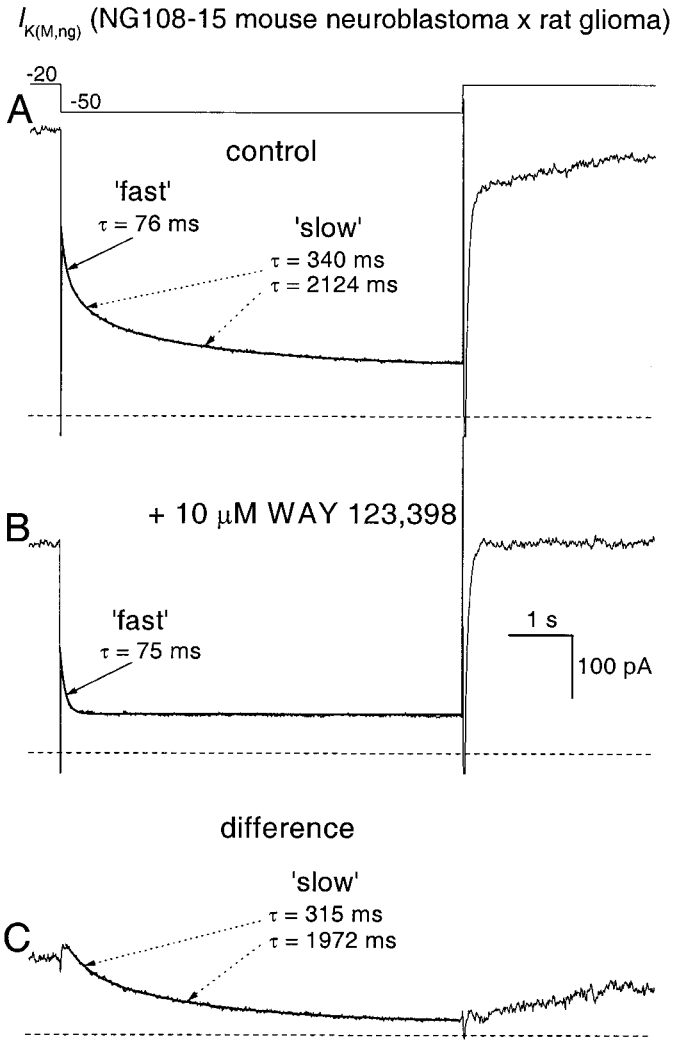

Figure 2. Kinetic analysis of the M-like current in a NG108–15 mouse neuroblastoma x rat glioma cell. Total $I_{K(M,ng)}$ was activated by holding at −20 mV and then deactivated by a 6 sec step (*top record*) to −50 mV before (*A*) and after (*B*) addition of the *erg*-channel blocker WAY 123,398 (10 μM). In control (*A*) the deactivation tail was fitted (*smooth line*, superimposed) by the sum of fast (τ = 76 msec, 254 pA) and two slow (τ = 340 msec, 37 pA and 2124 msec, 70 pA) exponential curves. WAY 123,398 abolished both slow components without affecting the fast component (*B*, τ = 76 msec). *C,* Slow component obtained by subtracting the record shown in *B* from that shown in *A* was fitted (*smooth line*, superimposed) by the sum of two kinetic components (τ = 315 and 1972 msec). All records were obtained from the same cell. *Dashed lines* denote zero current levels.

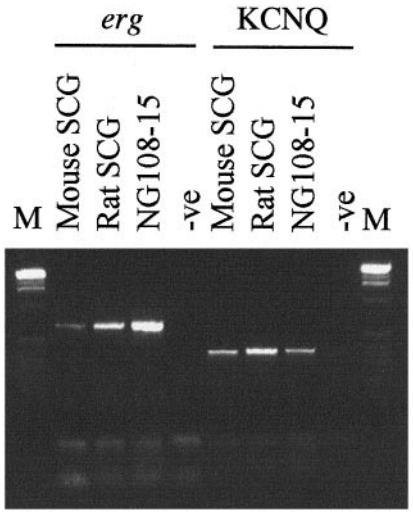

Figure 3. cDNA from mouse SCG, rat SCG, and chemically differentiated NG108–15 cells, was amplified using primers to the *erg* family of potassium channel genes or primers recognizing *KCNQ2* and *KCNQ3* potassium channel genes. Amplified products were obtained from all cell types but not from a negative control containing no template, indicating that members of these families are expressed by these cells. Sequence analysis revealed that the amplified product obtained from NG108–15 cDNA with primers to the *erg* genes was predominantly, if not exclusively, merg1. Analysis of the amplified product obtained using the *KCNQ* primers in both rat SCG and NG108–15 has shown these cells express both *KCNQ2* and *KCNQ3*. M-1 kb ladder DNA size standards.

receptors were maintained in culture as described in Mullaney et al. (1993). Superior cervical ganglion neurons were prepared as described previously (Owen et al., 1990) from 6-week-old C57 mice and 14-d-old Sprague Dawley rats, and used after 1–2 d in culture. Recordings from all three types of cell were made at room temperature (20–22°C), under identical experimental conditions (solutions, pipettes, etc.).

Culture and transfection of CHO hm1 cells. CHO hm1 cells are CHO-K1 cells, previously transfected with the human M_1 receptor (Mullaney et al., 1993). Cells were grown in 50 ml flasks at 37°C and 5% CO_2. The culture medium was α-MEM supplemented with 10% fetal calf serum, 1% L-glutamine, and 1% penicillin/streptomycin. Cells were split twice weekly when confluent, plated in 35 mm dishes, and transfected 1–2 d after plating using "LipofectAmine Plus" (Life Technologies, Gaithersburg, MD) according to the manufacturer's recommendations. Plasmids containing merg1a and CD8 cDNAs, both driven by cytomegalovirus promoter, were cotransfected in a ratio of 10:1. Cells for patch clamping were identified by adding CD8-binding Dynabeads (Dynal, Great Neck, NY) the day after transfection. For immunocytochemistry, a plasmid containing cDNA for jellyfish green fluorescent protein (GFP) was used as a marker for transfection.

Reverse transcription PCR. RNA was extracted from cell lines and superior cervical ganglia (SCG) using RNAzol B (Biogenesis Ltd.) and reverse-transcribed using oligo-dT and mouse murine leukemia virus reverse transcriptase (Promega, Madison, WI). The oligonucleotides used to amplify the *erg* gene family were: *erg-s* 5′ CCCYTTCAAGGCMGTGTGGG and *erg-a* 5′ CTGGTHAGRCTGCTGAAGGT. Primers were designed such that the amplified product spanned at least one intron to ensure amplification products were not derived from contaminating genomic DNA. The primers used for *KCNQ* PCR were *KCNQs* 5′ACCTGGARGCTBCTGGCTC and *KCNQa* 5′CCKCTYTTCTCAAAGTGCTTCTG. These primers were designed to amplify both *KCNQ2* and *KCNQ3* sequences. Cycling conditions were 95°C for 5 min and then 30 cycles of 95°C for 30 sec; 60°C for 1 min and 72°C for 1 min followed by a final step of 72°C for 10 min. Aliquots of the reaction mixture were visualized on a 2% (w/v) Metaphor agarose (FMC BioProducts, Rockland, ME). PCR products were cloned using the pGEM-T vector (Promega) and recombinant plasmids sequenced using *Taq* polymerase, fluoresceinated dye terminators and an Applied Biosystems 377 automated DNA sequencer.

Immunocytochemistry. This was performed using antibodies raised against synthetic peptides corresponding to the last 14 amino acids of the C-terminal fragment of merg1 (merg1-CT) and the first 17 amino acids of merg1b (merg1-NT), respectively. NG108–15 cells were seeded onto polyornithine-coated glass coverslips to allow immunocytochemistry. NG108–15 cells were washed in TBS (5.5 mM Tris, pH 7.4, and 137 mM NaCl) and fixed in acetone for 20 min at room temperature. The fixed cells were then treated with normal swine serum (1:10) in TBS for 30 min. Once excess serum was removed, the merg1-CT primary antibody was applied at 1:1000 dilution for 1 hr at room temperature. Different concentrations of the primary antibody were tested to optimize immunochemical labeling and minimize nonspecific staining of the tissue background. Bound antibodies were then detected using alkaline phosphatase-conjugated secondary antibodies (1:500; Dako, Carpinteria, CA), largely as described in Abogadie et al. (1997). Transfected mammalian CHO cells were briefly washed with PBS and fixed for 20–30 min in PBS containing 4% paraformaldehyde. Fixed cells were then rinsed

with PBS, blocked for 10 min with BSA, and permeabilized with 0.1% Triton X-100 for 5 min. Incubation with the anti-merg1 antibody and labeling were carried out as described for the NG108–15 cells.

Perforated-patch whole-cell recording. Cells were bath-perfused with the solution of the following composition (in mM): 144 NaCl, 2.5 KCl, 2 $CaCl_2$, 0.5 $MgCl_2$, 5 HEPES, and 10 glucose, pH 7.4, with Tris base. Pipettes were filled with the "internal" solution containing 90 mM K acetate, 20 mM KCl, 40 HEPES, 3 $MgCl_2$, 3 mM EGTA, and 1 mM $CaCl_2$. The pH was adjusted to 7.4 with NaOH. Amphotericin B was used to perforate the patch (Rae et al., 1991). The series resistance was not compensated because the error introduced was reasonably small. Thus, with the electrodes used (2–3 MΩ), the series resistance was 6–8 MΩ, and most of the currents were <0.5 nA, so the voltage error would be <5 mV. As confirmation that the voltage error was small, no correlation was found between deactivation time constants and initial current amplitude.

Data acquisition and analysis. Data were acquired and analyzed using pClamp software (version 6.0.3). Currents were recorded using an Axopatch 200A (or 200) patch-clamp amplifier, filtered at 1 kHz, and digitized at 1–4 kHz. In current-clamp experiments, currents were injected, and membrane potential was recorded using an Axoclamp-2 amplifier. Activation curves were fitted by the Boltzmann equation: $I/I(50) = 1/(1 + \exp(V_{1/2} - V)/k)$, where I is current at the test potential (estimated from the amplitudes of exponentials backfitted to the beginning of the test step), $I(50)$ is current at +50 mV, $V_{1/2}$ is the membrane potential, V, at which I is equal to ½ $I(50)$. Inhibition of the current was measured from the change in the amplitude of the deactivation tail recorded at −50 mV. Each tail was fitted by one or more exponentials, and the tail amplitude was taken as the sum of the amplitudes of all components contributing to it after backfitting them to the beginning of the hyperpolarizing pulse. In cells that had the *erg*-type component, backfitting was necessary to exclude not only the (relatively fast) capacity transient, but also the brief rising phase of the tail caused by the deinactivation of *erg*-type channels. To include the fast component (when present) in the fit, we had to position the fitting cursor earlier in the trace than was appropriate for the pure erg current. This tends to skew the τ values obtained for the *erg* components to larger values. This may explain the difference in slow τ values between the total and WAY 123,398-sensitive currents (Table 1). Inhibition curves were fitted by the Hill equation: $Y = Y_{max} * x^{nH}/(x^{nH} + IC_{50}{}^{nH})$, where Y_{max} is the maximum inhibition, x is the blocker concentration, n_H is the slope (Hill coefficient), and IC_{50} is the concentration corresponding to the half-maximal inhibition. Individual currents were measured and fitted using the Clampfit software, whereas the program "Origin" (version 5.0, Microcal Software) was used for fitting activation and inhibition curves and for creating the figures.

Drugs and chemicals. Linopirdine (DuP 996) was obtained from Research Biochemicals (Natick, MA). WAY 123,398 and azimilide were kindly provided by Wyeth-Ayerst Research (Princeton, NJ) and Dr. A. Busch (DG Cardiovascular, Frankfurt, Germany), respectively. All other drugs and chemicals were obtained from Sigma or BDH Chemicals (Poole, UK).

RESULTS

Fast and slow M-like ($I_{K(M,ng)}$) currents in NG108–15 mouse neuroblastoma x rat glioma cells

We recorded M-like currents ($I_{K(M,ng)}$) from 101 chemically differentiated NG108–15 cells using perforated-patch electrodes. Cells were carefully selected for their "neuron-like" appearance, i.e., large size and well-developed neuropil (Robbins et al., 1992). When studied with the conventional M-current voltage protocol, that is, by stepped hyperpolarization after predepolarization to approximately −20 mV (see Materials and Methods), currents showed characteristic M-like deactivation tails. However, the time course of these tail currents varied considerably from one cell to another. Figure 1 illustrates two extreme examples of this variation. Thus, in Figure 1*A*, deactivation during a 6 sec hyperpolarizing step was very slow, with an apparent "time-constant" of ~2 sec, whereas in Figure 1*B*, deactivation was complete within 2 sec.

Because a number of tumor cells (including neuroblastoma cells) have been reported to express *HERG*-like currents with

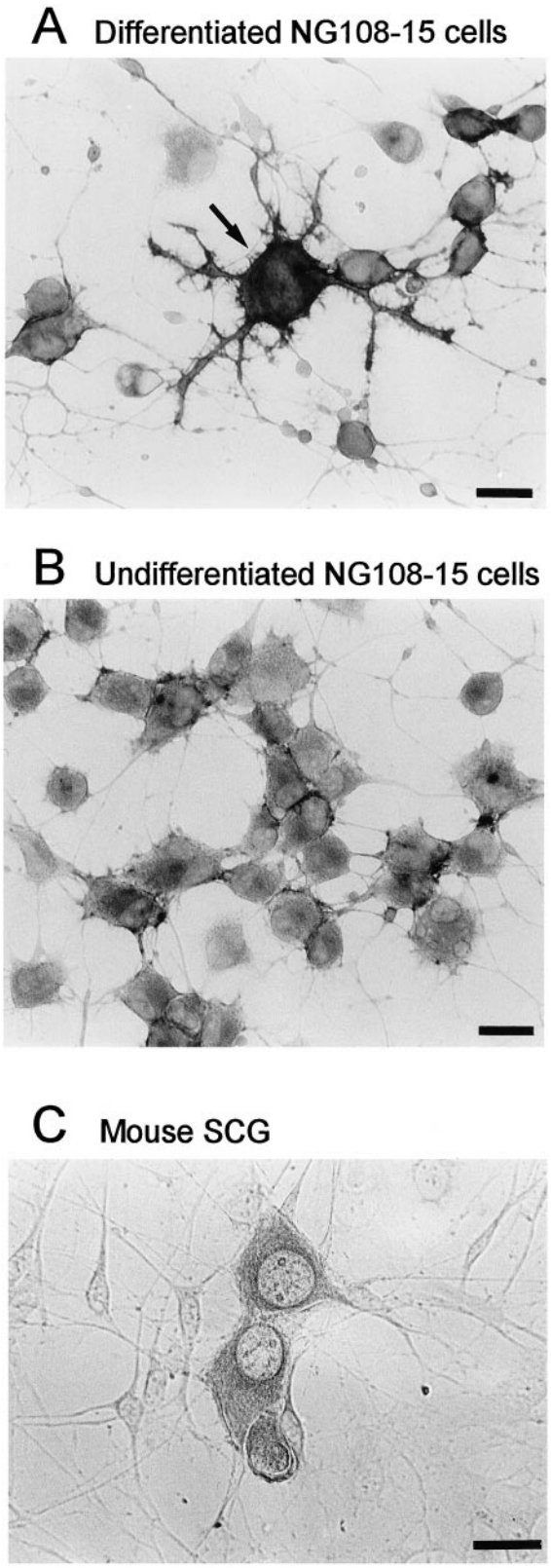

Figure 4. Immunocytochemical detection of merg1 protein in differentiated NG108 cells. Immunostaining for the C terminus of merg1 in chemically differentiated (*A*) and undifferentiated (*B*) NG108 cells, and in dissociated mouse SCG cells (*C*). Note that in *A*, a large NG108–15 cell (*arrow*) showed labeling of strong intensity, whereas adjacent smaller and bipolar cells were not stained. Micrographs were obtained using bright-field optics. Scale bars, 20 μm.

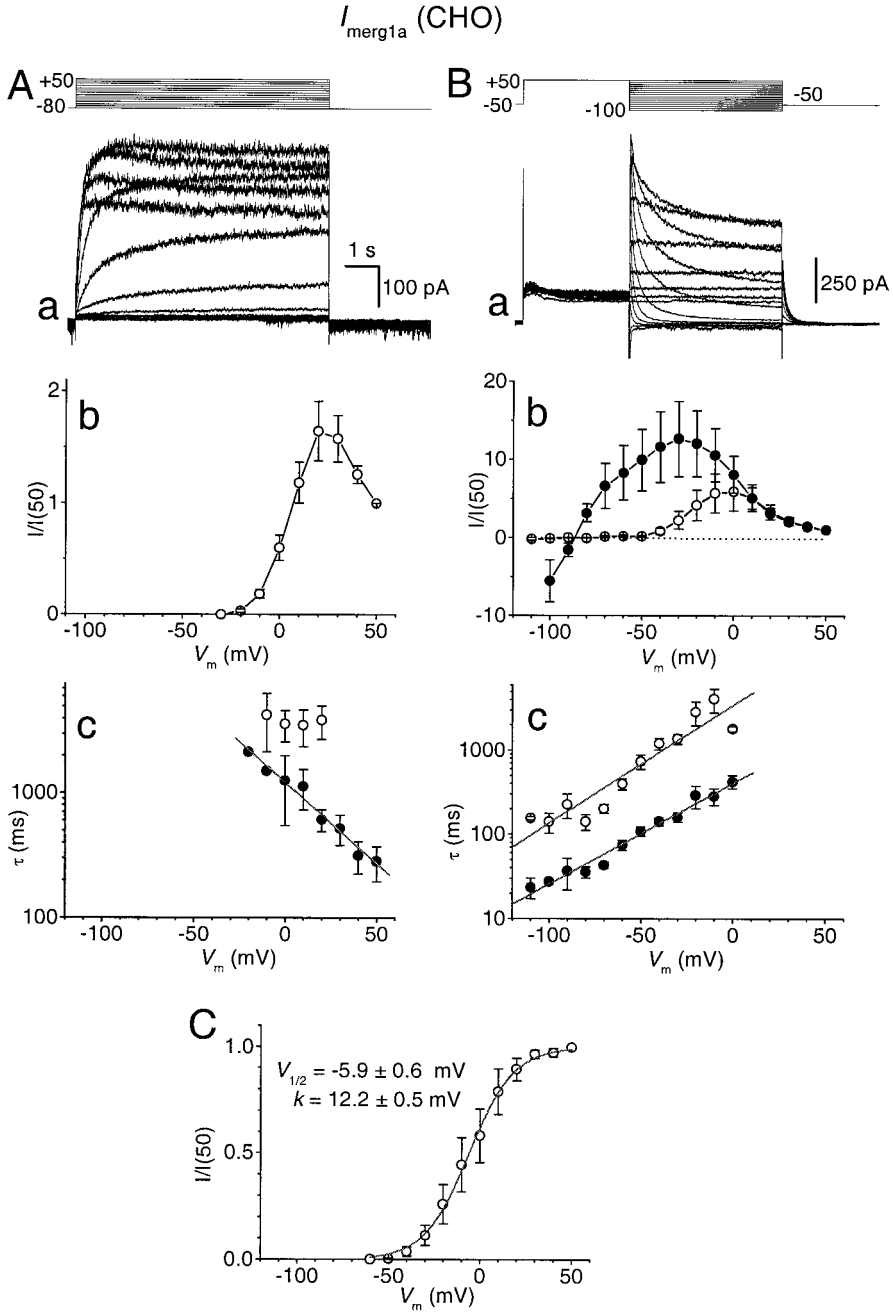

Figure 5. Characteristics of the merg1a current (I_{merg1a}) expressed in CHO cells. I_{merg1a} was activated by long (8 sec) depolarizing voltage steps from the holding level of −80 mV (*Aa*) and deactivated by hyperpolarizing steps after its full activation by a prepulse to +50 mV (*Ba*). Leak-subtracted steady-state *I–V* relationships obtained at the end of the depolarizing and hyperpolarizing pulses, respectively, are shown in *Ab* and *Bb* (*open circles*), and an "instantaneous" *I–V* relationship obtained at the beginning of the hyperpolarizing pulses for current deactivation is shown in *Bb* (*filled circles*). Activation (*Ac*) and deactivation (*Bc*) time constants were plotted semilogarithmically, and τ–*V* relationships were fitted by straight lines with τ at 0 mV and the slope equal to 1218 ± 1 msec and −0.013 ± 0.001 mV^{-1} in *Ac* and 403 ± 1 msec and 0.012 ± 0.0006 mV^{-1} (*filled circles*) and 3437 ± 1 msec and 0.014 ± 0.002 mV^{-1} (*open circles*) in *Bc*. *C,* Activation curve fitted by the Boltzmann equation at $V_{1/2}$ = −5.9 ± 0.6 mV and k = 12.2 ± 0.5 mV. Records in *Aa* and *Ba* were from the same cell. In *Ab, Ac*, *Bb, Bc,* and *C* the mean data are shown (*vertical lines* indicate SEMs) obtained from six and nine cells, respectively.

relatively slow rates of deactivation (Bianchi et al., 1998), we wondered whether these might contribute to the long deactivation tails. We tested this pharmacologically, using the *HERG* channel-blocking drug WAY 123,398 (Spinelli et al., 1993; Faravelli et al., 1996). As shown in Figure 1*A*, 10 μM WAY 123,398 blocked most of the long deactivation, leaving a residual fast component which was then eliminated by the M channel-blocking drug linopirdine (Aiken et al., 1995; Lamas et al., 1997). In contrast, the fast-deactivating current in Figure 1*B* was strongly blocked by linopirdine, leaving a slower component that was blocked in turn by WAY 123,398. Thus, comparison of the linopirdine- and WAY-sensitive currents (Fig. 1, *inserts*) showed that in fact each cell had two components to the deactivation currents, fast and slow, and that the overall time course of current deactivation was determined by their proportion. Furthermore, both components contributed to the sustained current recorded at −20 mV.

Because 10 μM WAY 123,398 produces a complete block of *erg* channels without affecting other K^+ channels such as sympathetic neuron M channels (see below), we analyzed the fast and slow components of the deactivation tails in more detail by recording currents in the absence and presence of WAY 123,398. Figure 2 exemplifies the results obtained in 86 of 101 cells so examined. Here, the control current recorded in the absence of WAY 123,398 (Fig. 2*A*) showed three components, a fast component with a time constant of 76 msec, and a slower, biexponential component with time constants of 340 msec and 2.1 sec. WAY 123,398 (Fig. 2*B*) eliminated the slower component, leaving only the fast component (τ, 75 msec), whereas the difference (WAY-sensitive) current (Fig. 2*C*) showed only the biexponential slow component (τ, 315 msec and 2.0 sec). Thus, the time constants of the residual current recorded after application of WAY 123,398 and of the subtracted (WAY-sensitive) current accurately repro-

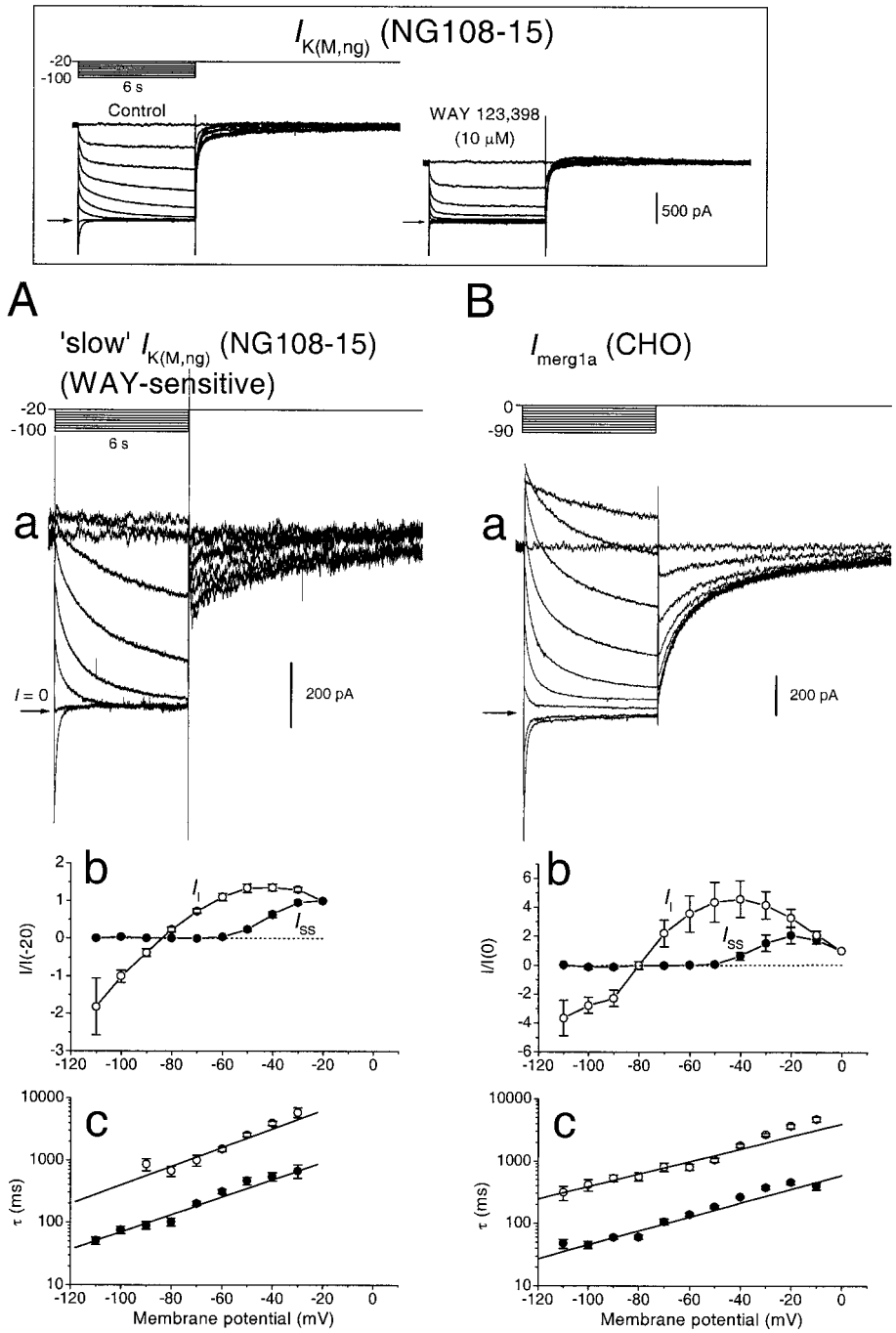

Figure 6. Comparison of the slow M-like ($I_{K(M,ng)}$) current in NG108–15 mouse neuroblastoma x rat glioma cells (*A*) and mouse-erg1a current (I_{merg1a}) expressed in CHO cells (*B*). The slowly deactivating component of $I_{K(M,ng)}$ (*Aa*) was recorded in response to long hyperpolarizing steps (holding level, −20 mV; step duration, 6 sec; interval, 60 sec; increment, −10 mV). These slow $I_{K(M,ng)}$ currents were obtained by subtracting the currents recorded in the presence of 10 μM WAY 123,398 (*box, right*) from those in the absence of the blocker (*box, left*). For comparison (*Ba*), I_{merg1a} is shown, obtained with a similar voltage protocol (note the holding potential of 0 mV in *Ba*). Deactivation tails were fitted by double-exponential curves (*smooth lines*, superimposed). Leak-subtracted steady-state (*filled circles*) and instantaneous (*open circles*) *I–V* relationships for $I_{K(M,ng)}$ (*Ab*) and I_{merg1a} (*Ba*) were obtained by measuring the current at the beginning and end of the voltage pulse. Fast (*filled circles*) and slow (*open circles*) time constants for deactivation of $I_{K(M,ng)}$ (*Ac*) and I_{merg1a} (*Bc*) were plotted semilogarithmically against membrane potential, and τ–*V* relationships were fitted by straight lines with τ at 0 mV and the slope equal to 2134 ± 1 msec and 0.015 ± 0.0009 mV^{-1} (*filled circles*) and 15737 ± 1 msec and 0.016 ± 0.002 mV^{-1} (*open circles*) in *Ac* and 680 ± 1 msec and 0.011 ± 0.0008 mV^{-1} (*filled circles*) and 5432 ± 1 msec and 0.012 ± 0.0007 mV^{-1} (*open circles*) in *Bc*. In *Ab, Ac, Bb,* and *Bc* the mean data are shown (*vertical lines* indicate SEMs) obtained from 26 and 29 cells, respectively.

duced the fast and slow components of the composite initial current. In this cell, the fast and slow components contributed 70 and 30%, respectively of the total tail current, and both contributed to the steady outward current at the holding potential as judged from the effect of WAY 123,398 on the holding current. On average, in the 86 cells expressing both currents, the fast- and slow-deactivating components contributed ~33 and 67%, respectively, to the total tail current (Table 1). In the other 15 cells, the tail current showed only the slowly deactivating component and was fully suppressed by WAY 123,398.

mRNAs for *merg1* and *KCNQ2* and *KCNQ3* in NG108–15 cells

The clearly distinguishable effects of linopirdine and WAY 123,398 on the tail currents illustrated in Figures 1 and 2 suggested that these might be composite currents, resulting from the deactivation of two different species of K^+ channel: one composed of linopirdine-sensitive *KCNQ2/3* subunits, or homologs thereof (Wang et al., 1998), and the other comprising a member (or members) of the *erg* family. We therefore sought evidence for the presence of transcripts of these channels by RT-PCR (see Materials and Methods). Transcripts for both *erg* and *KCNQ2/3* were detected (Fig. 3).

Sequence analysis of 10 independent clones from the erg PCR showed that each clone contained erg1 DNA sequence (data not shown), suggesting that these cells express predominantly, if not exclusively, *merg1* transcript (London et al., 1997). The *KCNQ2/3* transcript contained mRNA for both *KCNQ2* and *KCNQ3*. It may be noted in Fig. 3 that these transcripts were also present in

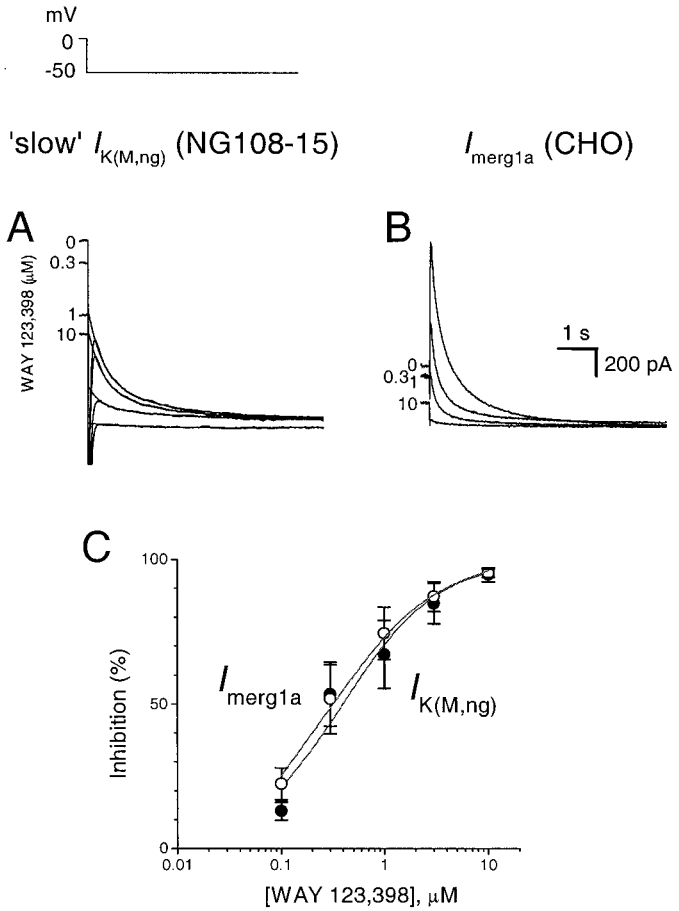

Figure 7. The slow component of the NG108–15 M-like current and the merg1a current are equally sensitive to WAY 123,398. Records in *A* and *B* show the slow component of $I_{K(M,ng)}$ and I_{merg1a} deactivation tail currents recorded on stepping from 0 to −50 mV in the presence of increasing concentrations of WAY 123,398 (0, 0.3, 1, and 10 μM). Plots in *C* show mean percent inhibition of the tail currents (*open circles*, $I_{K(M,ng)}$; $n = 4$; *filled circles,* I_{merg1a}; $n = 6$). See Table 2 for fitted parameters.

dissociated neurons from mouse and rat SCG (see also Shi et al., 1997; Wang et al., 1998).

Merg1 protein expression in chemically differentiated NG108–15 cells

The presence of mRNA transcripts does not necessarily correlate with translated protein products. We therefore tested for the expression of merg1a protein in NG108 cells by immunocytochemistry using a specific antibody raised against the C-terminal fragment of merg1 (merg1-CT; see Materials and Methods). As a control for specificity, the *merg1*-CT primary antibody was preincubated overnight with a 10-fold molar excess of the immunogenic peptide. Figure 4, *A* and *B,* compare merg1 immunolabeling in chemically differentiated and nondifferentiated NG108–15 cells, respectively. Strong labeling was observed in both cell bodies and neuropil of most large chemically differentiated NG108–15 cells of the type we normally selected for electrophysiological recording, whereas smaller cells with less well-developed processes showed weak or no immunoreactivity. No staining was observed in cells treated with preabsorbed antibody. Nondifferentiated cells, which normally expressed very small $I_{K(M,ng)}$, showed moderate or no staining. Interestingly, no staining was observed in dissociated mouse SCG neurons (Fig. 4*C*), or over the underlying glial cell layer. This latter (negative) finding accords with the absence of any effect of WAY 123,398 on membrane currents recorded from these neurons (see below). Also, no immunostaining of differentiated NG108–15 cells was detected after exposure to an antibody raised against an N-terminal sequence unique to the short form of merg1 (merg1b), the expression of which is restricted to cardiac cells (London et al., 1997). This suggests that the protein tagged by the C-terminal antibody is the product of the long-form transcript merg1a (London et al., 1997; see also below).

Strong immunoreactivity for merg1-CT antibody was also detected in CHO cells transfected with merg1a cDNA. No staining was observed in untransfected cells, in cells transfected only with the GFP plasmid, or in cells treated with preabsorbed antibody (data not shown).

Slow $I_{K(M,ng)}$ is mimicked by merg1a current (I_{merg1a}) expressed in CHO cells

The above results suggested that the slow component of the M-like current in NG108–15 cells might well be carried by merg1a channels. We tested this further by expressing merg1a cDNA in mammalian CHO cells. Figure 5 illustrates the resultant membrane currents. I_{merg1a} was activated by membrane depolarization to equal or positive to −40 mV, but showed substantial inactivation during the (long) depolarizing command at potentials positive to 0 mV (Fig. 5*Aa*). As a result, the "steady-state" current–voltage curve was "bell-shaped" (Fig. 5*Ab*). The time course of this composite activation (accompanied by inactivation) could be described by two exponentials, accelerating strongly with depolarization (Fig. 5*Ac*). When the cell was hyperpolarized after a depolarizing prepulse to +50 mV, there was a large transient enhancement of the current, caused by removal of channel inactivation, followed by a slower deactivation (Fig. 5*Ba,b*). Two deactivation components were detected that were strongly shortened by membrane hyperpolarization (Fig. 5*Bc*). The mean activation curve deduced from tail currents followed a Boltzmann equation with $V_{1/2} = -5.9 \pm 0.6$ mV and $k = 12.2 \pm 0.5$ mV (Fig. 5*C*). However, when individual curves were fitted, they showed a great variation in $V_{1/2}$ (range, between −27 and 13 mV; $n = 9$) and small variation in k (range, between 6.9 and 10). These results accord well with previous observations on merg1a currents in oocytes (London et al., 1997).

We next compared the properties of I_{merg1a} deactivation more closely with those of the WAY-sensitive slow component of $I_{K(M,ng)}$, using the "standard" M current protocol, that is, currents were preactivated by holding at the depolarized potential of 0 mV (−20 mV in the case of $I_{K(M,ng)}$, to avoid contamination by other, primarily Ca^{2+}-dependent, K^+ currents) and then deactivated by 6 sec step commands to various negative potentials. As shown in Figure 6, there was a close correspondence between the two. There were three main differences. First, deactivation of I_{merg1a} was preceded by a larger transient reactivation: this presumably reflected the greater steady-state inactivation of I_{merg1a} at 0 mV than that of slow $I_{K(M,ng)}$ at −20 mV. Second, the threshold for activation of I_{merg1a} was ~10 mV more positive than that for slow $I_{K(M,ng)}$ (Fig. 6*Ab*,*Bb*): the reason for this is not known but may simply relate to different cell types. Third, whereas both showed a biexponential deactivation, the time constants for the two components of I_{merg1a} deactivation measured at −50 mV were ~40% of those for deactivation of the slow $I_{K(M,ng)}$ measured at the same potential (Table 1). The time constants showed a comparable voltage dependence (Fig. 6,compare *Ac*, *Bc*), so this

Table 2. Effects of K^+ channel blockers on fast and slow $I_{K(M,ng)}$, I_{merg1a}, and $I_{K(M)}$

Blocker	Slow $I_{K(M,ng)}$	I_{merg1a}	Fast $I_{K(M,ng)}$	$I_{K(M)}$
WAY 123,398				
IC_{50} (μM)	0.4 ± 0.07	0.3 ± 0.02	no effect (10 μM)	no effect (10 μM)
n_H	1.0 ± 0.2	0.9 ± 0.07		
	(4)	(6)	(37)	(9)
Azimilide				
IC_{50} (μM)	6.5 ± 0.7	6.4 ± 0.3	31.1 ± 1.8	12.9 ± 0.7
n_H	0.9 ± 0.08	0.8 ± 0.03	0.9 ± 0.05	1.3 ± 0.09
	(5)	(4)	(4)	(3)
THA				
IC_{50} (μM)	11.5 ± 1.5	35.7 ± 9.7	1542 ± 200	1279 ± 75
n_H	0.6 ± 0.05	0.6 ± 0.1	0.7 ± 0.07	0.8 ± 0.03
	(3)	(7)	(3)	(4)
Linopirdine				
IC_{50} (μM)	>>30	>30	1.2 ± 0.02	3.5 ± 0.2
n_H			1.2 ± 0.03	0.8 ± 0.04
	(4)	(6)	(6)	(6)
TEA				
IC_{50} (mM)	16.7 ± 3.4	24.1 ± 3.6	1.1 ± 0.09	10.9 ± 0.7
n_H	0.8 ± 0.1	0.6 ± 0.1	0.6 ± 0.03	0.6 ± 0.02
	(6)	(3)	(5)	(4)
Ba^{2+}				
IC_{50} (μM)	134 ± 6	492 ± 57	248 ± 26	393 ± 36
n_H	1.0 ± 0.04	1.0 ± 0.1	0.9 ± 0.07	0.8 ± 0.05
	(3)	(5)	(3)	(3)

Mean ± SEM. Number of cells in parentheses. Inhibition constants (IC_{50}) were determined from dose–response curves of the type illustrated in Figures 7 and 9. Effects on fast and slow currents in NG108-15 cells were determined from kinetic analysis of deactivation tails as illustrated in Figure 2, supplemented (where appropriate) by tests after inhibiting the slow component with WAY 123,398, as in Figure 9.

difference may be explained by the different activation thresholds and/or the different size of the voltage step (in four CHO cells using a prepulse protocol, the first and the second slow deactivation τ values for I_{merg1a} were slower after a prepulse to −20 mV compared with a prepulse to 0 mV, by 41 and 57%, respectively).

For comparison, we also examined the properties of currents generated by the short "cardiac" isoform merg1b expressed in CHO cells (I_{merg1b}; $n = 3$; data not shown). Whereas the voltage dependence of I_{merg1b} activation and deactivation were very similar to that of the slow $I_{K(M,ng)}$ and of I_{merg1a}, both activation and deactivation of I_{merg1b} were several times faster (Table 1), as previously reported in oocytes by London et al. (1997) (see also Lees-Miller et al., 1997). Hence, and in accordance with the lack of antibody staining mentioned above and the absence of merg1b mRNA expression in the nervous system (London et al., 1997), it is unlikely that merg1b channels contribute to slow $I_{K(M,ng)}$.

Slow $I_{K(M,ng)}$ and I_{merg1a} show similar pharmacology

We next compared the sensitivity of the slowly deactivating component of the NG108–15 current $I_{K(M,ng)}$ with that of CHO-expressed merg1a currents to some blocking drugs. As shown in Figure 7, both tail currents were blocked by the anti-arrhythmic drug WAY 123,398 with equal facility (IC_{50} values, 0.4 and 0.3 μM, respectively; Table 2). They were also equally sensitive to another anti-arrhythmic drug, azimilide (IC_{50} values, 6.4 and 6.5 μM, respectively; Table 2; Busch et al., 1998). I_{merg1a} was also inhibited by 9-aminotetrahydroacridine (THA; IC_{50} value, 36 μM; Table 2), a compound that had previously proved unexpectedly potent in inhibiting the M-like current in NG108–15 cells (Robbins et al., 1992). In contrast, neither current was inhibited by the ganglionic M channel- and *KCNQ2/3* channel-blocking agent linopirdine at concentrations up to 30 μM [Noda et al. (1998) reported an IC_{50} of 36 μM against the NG108–15 current, but this was measured from the depression of the composite current, and the Hill slope was rather shallow, so probably reflected its primary action on the fast current component, see below]. Also, both currents were very insensitive to tetraethylammonium (TEA), with IC_{50} values of 17 and 24 mM (Table 2). Thus, I_{merg1a} provides a good match for the slowly deactivating component of $I_{K(M,ng)}$, both kinetically and pharmacologically.

Fast $I_{K(M,ng)}$ is mimicked by the M current ($I_{K(M)}$) in mouse sympathetic neurons

As noted above (Fig. 1), the fast component of $I_{K(M,ng)}$ was readily suppressed by 10 μM linopirdine. Since linopirdine blocks M currents in sympathetic ganglia (Lamas et al., 1997; Wang et al., 1998), this suggested that fast $I_{K(M,ng)}$ might correspond to the "true" (ganglionic-type) M current. We assessed this by comparing fast WAY-insensitive $I_{K(M,ng)}$ with the M current recorded from dissociated mouse SCG neurons. (We used *mouse* neurons because (1) the parent neuroblastoma to the NG108–15 hybrid cell line is derived from mouse neural crest; and (2) sequence analysis of the PCR products obtained with the *KCNQ* primers showed that NG108–15 cells expressed both the mouse KCNQ2 and the mouse KCNQ3. Because we have successfully used these primers to amplify the rat KCNQ2 and KCNQ3 genes, we conclude that NG108–15 cells express predominantly, if not exclusively, the mouse KCNQ genes.) Figure 8 shows families of fast $I_{K(M,ng)}$ (*Aa*) and $I_{K(M)}$ (*Ba*) activated by membrane depolariza-

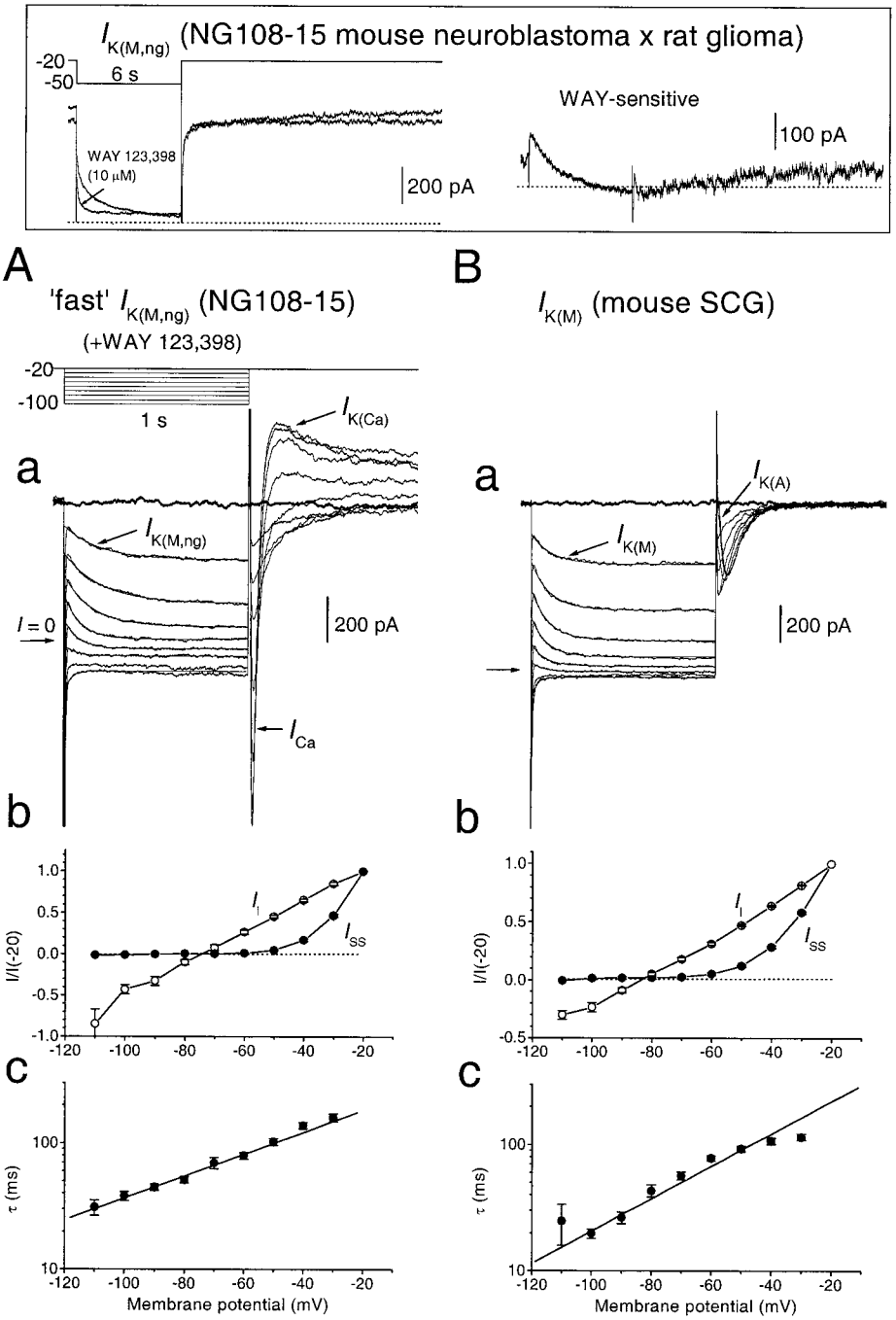

Figure 8. Characteristics of the fast M-like ($I_{K(M,ng)}$) current in a NG108–15 mouse neuroblastoma x rat glioma cell (*A*) and the M current ($I_{K(M)}$) in a mouse SCG neuron (*B*). The fast-deactivating component of $I_{K(M,ng)}$ (*Aa*) was recorded in the presence of 10 μM WAY 123,398 at different membrane potentials (holding level, −20 mV; step duration, 1 sec; interval, 10 sec; increment, −10 mV). *Box,* Inhibition of the slow, WAY-sensitive component in this cell: currents before and after application of 10 μM WAY 123,398, *left*, and the difference current, *right*. For comparison (*Ba*), $I_{K(M)}$ is shown, obtained with the same voltage protocol. Deactivation tails were fitted by single exponential curves (*smooth lines*, superimposed). Leak-subtracted steady-state (*filled circles*) and instantaneous (*open circles*) *I–V* relationships for $I_{K(M,ng)}$ (*Ab*) and $I_{K(M)}$ (*Ba*) were obtained by measuring the current at the beginning and end of the voltage pulse. When the time constants for deactivation of $I_{K(M,ng)}$ (*Ac*) and $I_{K(M)}$ (*Bc*) were plotted semilogarithmically against membrane potential, τ–*V* relationships were fitted by straight lines with τ at 0 mV and the slope equal to 271 ± 1 msec and 0.009 ± 0.0004 mV^{-1} in *Ac* and 399 ± 1 msec and 0.013 ± 0.0009 mV^{-1} in *Bc*. In *Ab, Ac, Bb,* and *Bc* the mean data are shown (*vertical lines* indicate SEM) obtained from 30 and 15 cells, respectively.

tion to −20 mV and deactivated by 1 sec hyperpolarizations at −30 to −100 mV. The slow component of $I_{K(M,ng)}$ was eliminated using 10 μM WAY 123,398, as shown in the box in Figure 8. Fast $I_{K(M,ng)}$ and $I_{K(M)}$ had similar voltage dependences (Fig. 8*A,B*) to each other, and also to slow $I_{K(M,ng)}$ and I_{merg1a} (compare Fig. 6). However, unlike slow $I_{K(M,ng)}$, deactivation tails of fast $I_{K(M,ng)}$ and mouse $I_{K(M)}$ were fitted with single exponential curves: these had time constants similar to each other but much shorter than those in the slow $I_{K(M,ng)}$ and I_{merg1a} (Table 1).

Pharmacological comparison of fast $I_{K(M,ng)}$ and mouse $I_{K(M)}$

Like fast $I_{K(M,ng)}$, mouse $I_{K(M)}$ was unaffected by 10 μM WAY 123,398. $I_{K(M)}$ recorded from 5 rat SCG neurons was also insensitive to this compound. Furthermore, both fast $I_{K(M,ng)}$ and mouse $I_{K(M)}$ were 1.5–2 orders of magnitude less sensitive to THA than were slow $I_{K(M,ng)}$ or I_{merg1a} (IC_{50} values, 1.5 and 1.3 mM; Table 2). This accords with the relative insensitivity of rat SCG $I_{K(M)}$ to THA reported previously (Marsh et al., 1990). Figure 9 shows the responses of fast $I_{K(M,ng)}$ and mouse $I_{K(M)}$ to linopirdine and TEA. Whereas both currents were considerably more sensitive than slow $I_{K(M,ng)}$ or I_{merg1a} to linopirdine, the neuroblastoma–glioma current was clearly more sensitive than the mouse SCG current (IC_{50} values, 1.2 and 3.5 μM, respectively; Table 2). Likewise, fast $I_{K(M,ng)}$ was more readily blocked than the mouse $I_{K(M)}$ by TEA (see Discussion). Nevertheless, although not completely identical pharmacologically, fast $I_{K(M,ng)}$ and

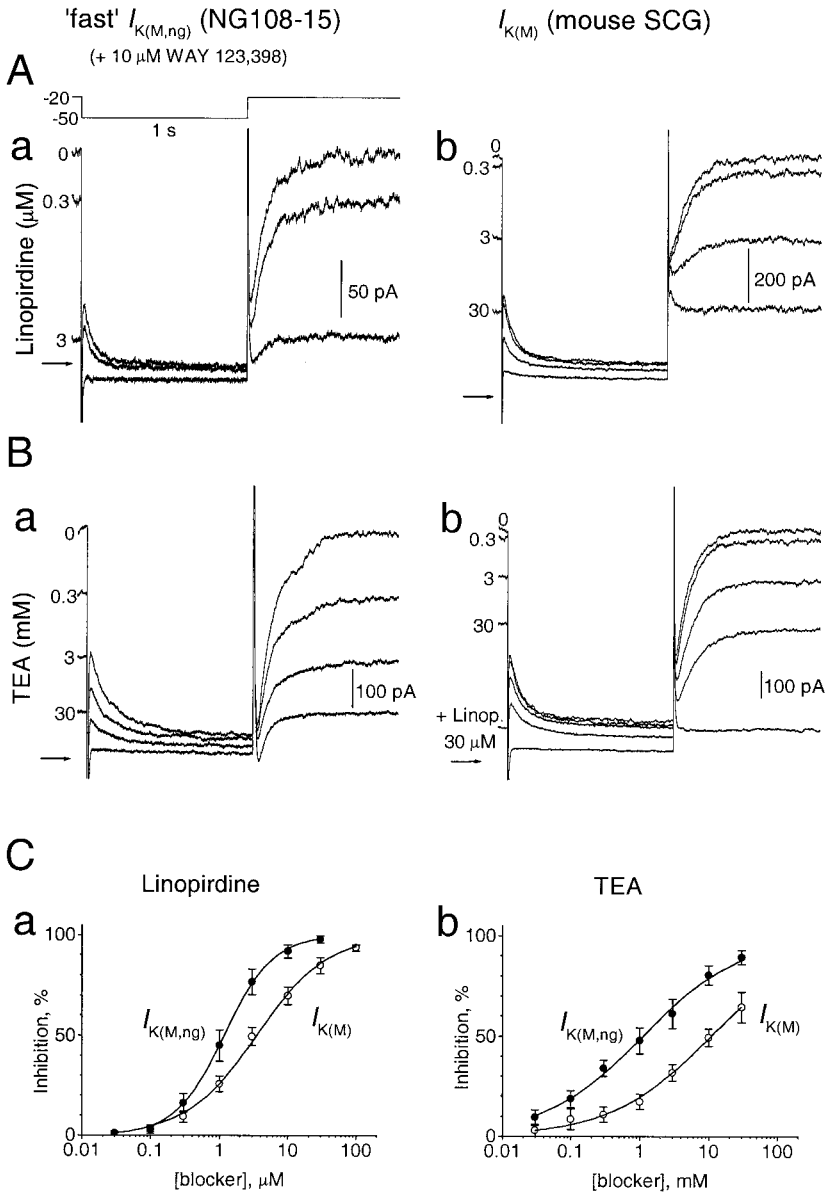

Figure 9. Differential sensitivities of fast $I_{K(M,ng)}$ and $I_{K(M)}$ to linopirdine and TEA. The fast (WAY-insensitive) component of $I_{K(M,ng)}$ and $I_{K(M)}$ was recorded in response to 1 sec steps from the holding level of −20 to −50 mV, in the absence and presence of different concentrations of linopirdine (*Aa, Ab*) and TEA (*Ba, Bb*). *C,* Concentration dependences of inhibition of the two currents by linopirdine (*a*) and TEA (*b*). *Smooth lines* are the fits by the Hill equation. For the parameters of the fit see Table 2.

mouse SCG $I_{K(M)}$ are clearly similar and together show an obvious difference from slow $I_{K(M,ng)}$ and I_{merg1a}.

Both fast and slow $I_{K(M,ng)}$, and I_{merg1a}, are inhibited through activation of M1 muscarinic receptors

Activation of M_1 muscarinic receptors inhibits both the total (composite) M-like current ($I_{K(M,ng)}$) in NG108–15 cells (Fukuda et al., 1988; Robbins et al., 1991, 1993), and the M current $I_{K(M)}$ in rat (Marrion et al., 1989; Bernheim et al., 1992) and mouse (Hamilton et al., 1997) sympathetic neurons. We therefore examined the effects of a muscarinic stimulant, oxotremorine-M (Oxo-M; 10 μM), on each component of $I_{K(M,ng)}$, as well as I_{merg1a}, in M_1 muscarinic receptor-transformed NG108–15 and CHO cells. Figure 10 shows that Oxo-M inhibited the slow $I_{K(M,ng)}$ (*A*) and I_{merg1a} (*B*). Such inhibitions were observed in seven of eight NG108–15 cells (mean inhibition, 42.3 ± 13.8%) and six of six merg1a-expressing CHO cells (mean inhibition, 50.7 ± 10.8%). Inhibition of both slow $I_{K(M,ng)}$ and I_{merg1a} was accompanied by a significant acceleration of their deactivation kinetics (Fig. 11): on average, the two components in slow $I_{K(M,ng)}$ and I_{merg1a} were shortened by 25.4 ± 10.0% and 34.6 ± 9.0% (n = 6) and 36.5 ± 4.8% and 27.8 ± 10.1% (n = 4), respectively.

Figure 12 shows examples of inhibitions of fast $I_{K(M,ng)}$ and mouse $I_{K(M)}$ by Oxo-M. Such inhibitions were observed in four of four NG108–15 cells (mean inhibition, 72.6 ± 13.8%; n = 4). As expected (Hamilton et al., 1997), similar inhibition was consistently observed in sympathetic neurons.

Fast and slow $I_{K(M,ng)}$ control firing in NG108–15 cells

The function of the M current is to act as a brake on repetitive firing. Thus, inhibition of the M current in sympathetic neurons, either by muscarinic agonists (Brown and Selyanko, 1985) or by an M channel-blocking agent (Wang et al., 1998), is associated with increased repetitive firing during depolarizing current injections. A similar effect has also been reported in M_1-transformed NG108–15 cells after application of a muscarinic agonist (Robbins et al., 1993). However, in the latter case, it is not clear whether this results from inhibition of the fast or slow $I_{K(M,ng)}$, or both. We tested this by injecting long (7 sec) depolarizing currents into NG108–15 cells and then observing the effects of

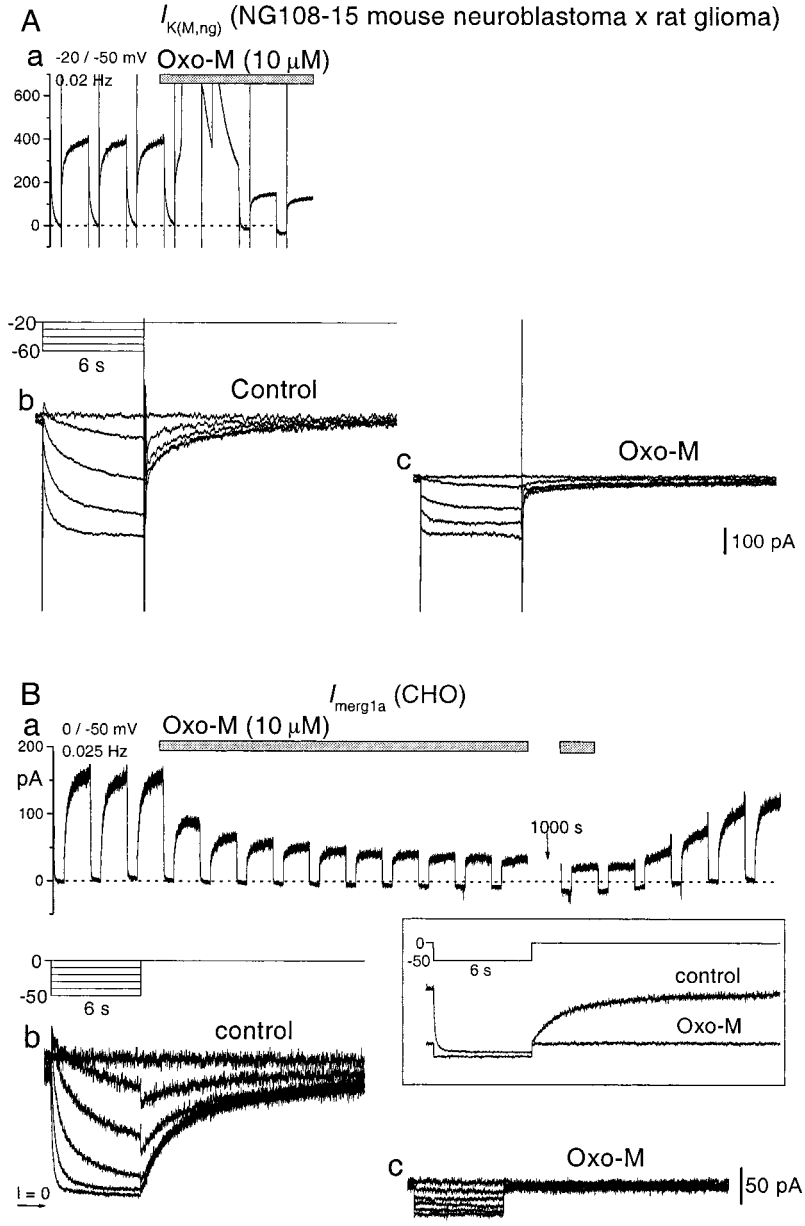

Figure 10. Muscarinic inhibition of slow $I_{K(M,ng)}$ in a NG108–15 mouse neuroblastoma x rat glioma cell (*A*) and I_{merg1a} expressed in a CHO cell (*B*). Currents (*Aa, Ba*) were produced by holding at −20 mV (*A*) or 0 mV (*B*) and giving repeated steps (at 0.02 Hz in *A* and 0.025 Hz in *B*) to −50 mV for 6 sec. Both steady-state currents at the holding potentials and deactivation currents at the test potential were reduced by bath-application of oxotremorine-M (*Oxo-M*; 10 μM). In an NG108–15 cell, inhibition of $I_{K(M,ng)}$ was preceded by a transient activation of a Ca^{2+}-activated K^+ current (*Aa*). Families of currents in *b* and *c* were obtained in response to incremental (−10 mV) hyperpolarizing voltage steps before (*b*) and during (*c*) action of Oxo-M. The *insert* in *B* shows superimposed current produced by voltage steps from 0 to −50 mV before and during the action of Oxo-M.

selectively inhibiting fast and slow $I_{K(M,ng)}$ with linopirdine and WAY 123,398, respectively. The depolarizing currents produced a short burst of repetitive firing in 20 of 22 NG108–15 cells tested and single action potentials in the remaining two cells. Figure 13 shows that 30 μM linopirdine (which blocked the fast current completely and inhibited the slow $I_{K(M,ng)}$ by only 33%) produced a strong reduction in spike adaptation, whereas 10 μM WAY 123,398 had a much weaker effect. Neither linopirdine nor WAY 123,398 had any effect on spike repolarization.

DISCUSSION

The main point emerging from this work is that the M-like current in NG108–15 cells ($I_{K(M,ng)}$) is a composite current generated by at least two channel types: a fast-deactivating set of channels similar (but not quite identical) to those carrying the M current in mouse sympathetic neurons and tentatively identified as *KCNQ2*/*KCNQ3* (Wang et al., 1998), and a slower-deactivating current probably formed from merg1a (London et al., 1997). *KCNQ2* and *KCNQ3* are analogs of *KCNQ1*, which coassembles with *KCNE* (minK) subunits to give the cardiac current I_{Ks} (the slow component of the cardiac "delayed rectifier"), and mutation of which causes one form of the cardiac long QT syndrome (Yang et al., 1997). *KCNQ2* and *KCNQ3* have so far been detected only in brain and ganglia, and are implicated in a form of juvenile epilepsy (Biervert et al., 1998; Charlier et al., 1998; Schroeder et al., 1998; Singh et al., 1998; Yang et al., 1998). Merg1a is one isoform of the mouse homolog of *erg*, originally cloned from a rat brain hippocampal cDNA library (Warmke and Ganetzky, 1994); mRNA for *erg* is found mainly in heart and brain (London et al., 1997; Wymore et al., 1997). Mutations of the human homolog *HERG* give rise to a cardiac long QT syndrome (Curran et al., 1995; Sanguinetti et al., 1996), whereas mutations in *Drosophila erg* are responsible for the seizure phenotype associated with hyperactivity in the flight motor pathway (Titus et al., 1997; Wang et al., 1997). Thus, both these channel types have been implicated

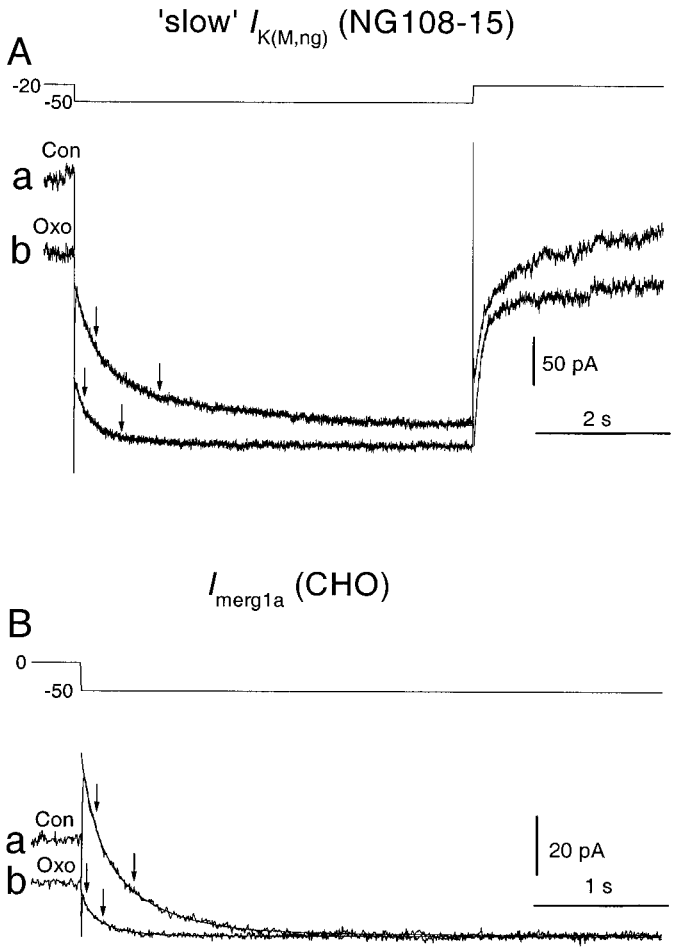

Figure 11. Muscarinic inhibition of slow $I_{K(M,ng)}$ in a NG108–15 mouse neuroblastoma x rat glioma cell (*A*) and I_{merg1a} expressed in a CHO cell (*B*) is accompanied by acceleration of their deactivation kinetics. Superimposed are deactivation tails obtained by stepping to −50 mV from −20 mV (*A*) or 0 mV (*B*) in control (*Con*) and in the presence of 10 μM oxotremorine-M (*Oxo*). *Smooth lines* are double-exponential fits with time constants (indicated by *arrows*) equal to 276 and 1271 msec (*Con*) and 176 and 708 msec (*Oxo*) in *A* and 92 and 398 msec (*Con*) and 71 and 290 msec (*Oxo*) in *B*.

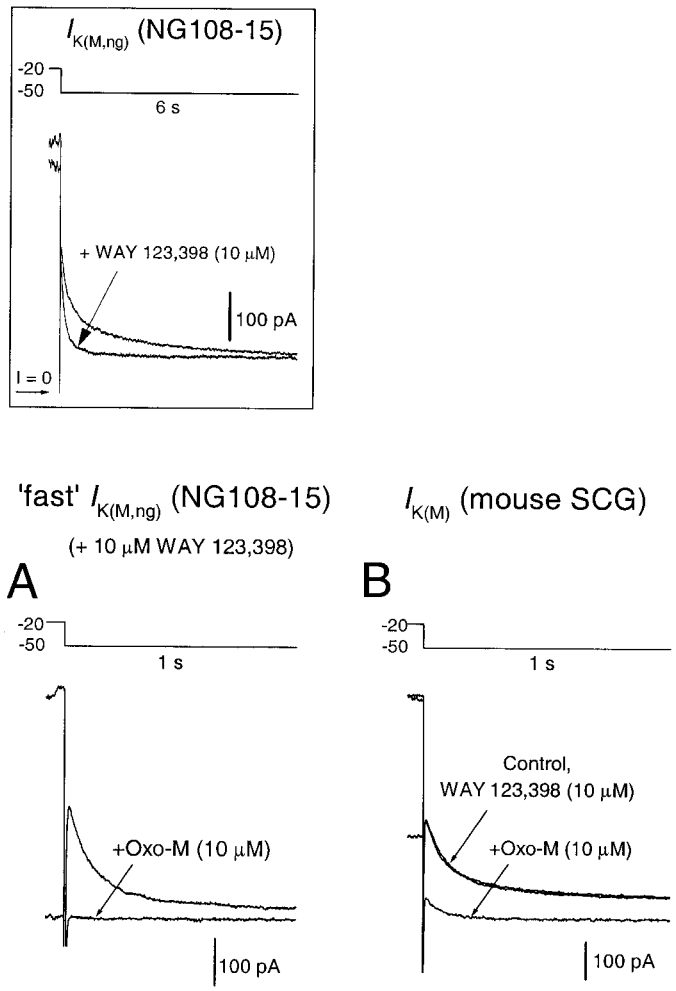

Figure 12. Muscarinic inhibition of fast $I_{K(M,ng)}$ in an NG108–15 mouse neuroblastoma x rat glioma cell (*A*) and $I_{K(M)}$ in a mouse sympathetic neuron (*B*). Fast-deactivating $I_{K(M,ng)}$ currents (*A*) are shown during 1 sec of hyperpolarization from −20 to −50 mV, before and during the action of oxotremorine-M (*Oxo-M*; 10 μM). Both currents were obtained in the presence of 10 μM WAY 123,398. (The effect of WAY 123,398 on the total $I_{K(M,ng)}$ recorded in this cell with a longer, 6 sec pulse, is shown in the *box*.) Currents in a mouse sympathetic neuron were obtained before and after addition of WAY 123,398 and WAY 123,398 + Oxo-M.

in the control of excitability *in vivo*. This is the first example of these two channels forming overlapping and functionally similar components of membrane current.

Our conclusion that two different channels are involved is based on: (1) the presence of mRNA transcripts and protein; (2) biophysical properties (voltage threshold and deactivation parameters); (3) sensitivity to potassium channel blockers; and (4) modulation of the channel by an agonist. Thus, we demonstrate the presence of mRNA and protein for *merg1*, and mRNA for *KCNQ2* and *KCNQ3*, in NG108–15 cells. We show that the kinetics of merg1a heterologously expressed in mammalian cells correspond closely to those of the slow $I_{K(M,ng)}$. We also show that the two are equally sensitive to the *merg*-selective blocking agents WAY 123,398 and azimilide, and insensitive to the ganglionic M current and *KCNQ2/3* channel-blocking agent linopirdine. On the other hand, we find that the fast $I_{K(M,ng)}$ kinetically matches the mouse SCG $I_{K(M)}$, that these two are pharmacologically similar (although not quite identical), and that they can be distinguished from both slow $I_{K(M,ng)}$ and I_{merg1a} by their greater sensitivity to linopirdine and insensitivity to WAY 123,398. We also show that both fast and slow components of $I_{K(M,ng)}$ are inhibited by stimulating M_1 muscarinic acetylcholine receptors and that the nature of the inhibition of these two components matches that for inhibition of mouse $I_{K(M)}$ and I_{merg1a}, respectively.

$I_{K(M)}$ in rat ganglion cells has been ascribed to current through channels composed of heteromultimeric assemblies of expressed *KCNQ2* and *KCNQ3* subunits (Wang et al., 1998). This may also be true for $I_{K(M)}$ in mouse ganglion cells and for the fast component of $I_{K(M,ng)}$ in NG108–15 cells, because we have found that both cell types show transcripts for these subunits. However, as yet, we cannot exclude a contribution from other, homologous, *KCNQ* subunits. Furthermore, fast $I_{K(M,ng)}$ was distinctly more sensitive to TEA and to linopirdine than was mouse ganglion $I_{K(M)}$, suggesting that the subunit composition of the presumed-*KCNQ* channels in these two cell types might differ.

The presence of functional merg1a channels in these cells is not, in itself, particularly surprising, because mRNA transcripts have been identified in a number of neuroblastoma-derived cells

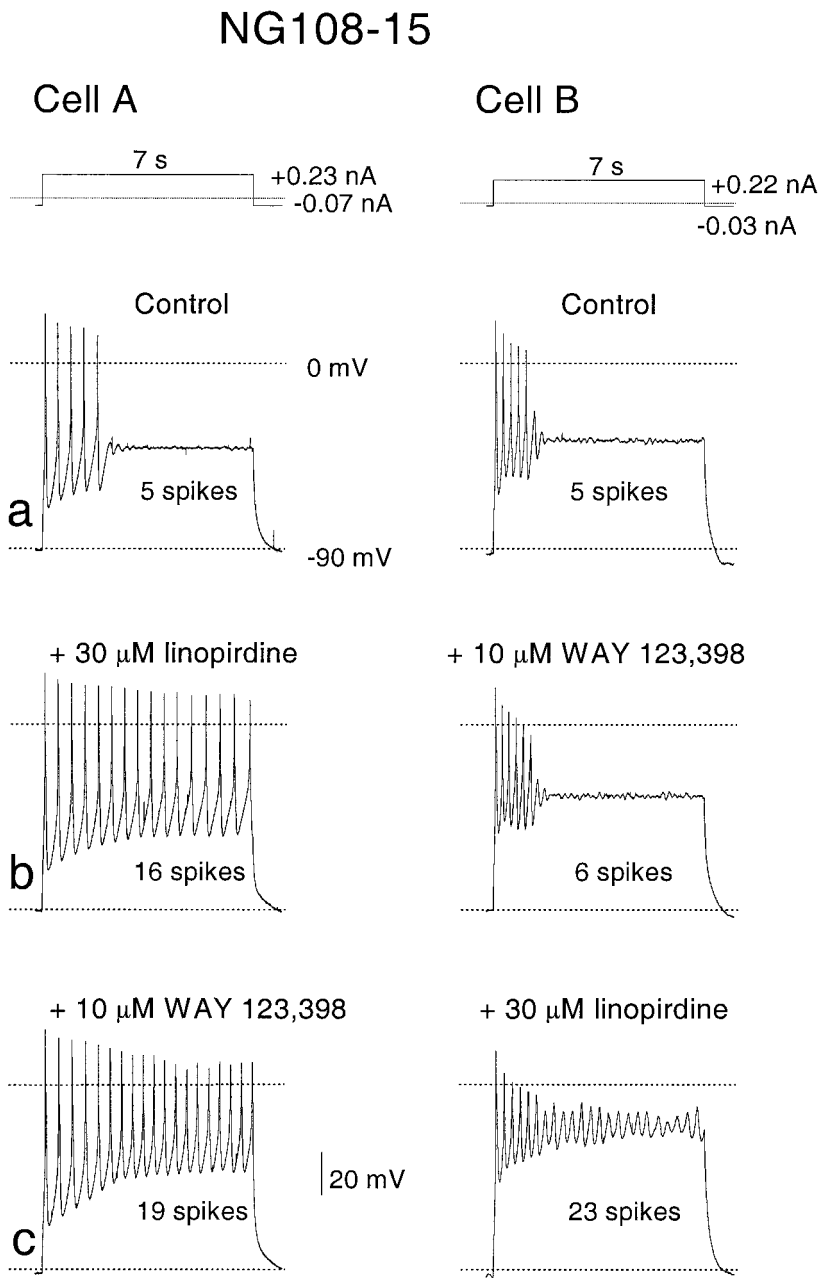

Figure 13. Effects of inhibiting fast and slow $I_{K(M,ng)}$ on firing in NG108–15 cells. Records show action potential trains in two NG108–15 cells (*A, B*) produced by long (7 sec) depolarizing pulses (*top records*) from the holding potential of −90 mV in the absence of drugs (*Aa, Ba*), in the presence of 30 μM linopirdine (*Ab*), 10 μM WAY 123,398 (*Bb*), or in the presence of both linopirdine and WAY 123,398 (*Ac, Bc*).

(including NG108–15) using probes to the human homolog *HERG* (Bianchi et al., 1998), and an "inwardly rectifying" current, retrospectively similar to an *erg* current, was reported in NG108–15 cells by Hu and Shi (1997) (see also Bianchi et al., 1998). However, in previous experiments, the properties of this current were mostly studied using solutions containing a raised K^+ concentration, so that its relation to the M-like current was difficult to discern. It is clear from the present experiments (using normal external K^+ concentrations) that the activation range of I_{merg1a} overlaps that of the true $I_{K(M)}$, but that deactivation of I_{merg1a} contributes a distinctive slow component to composite current deactivation; and furthermore, that the proportional contributions of I_{merg1a} and $I_{K(M)}$ to the total M-like current vary appreciably from cell to cell.

The merg1a and (presumed) *KCNQ* currents also overlap functionally. Thus, Chiesa et al. (1997) have provided evidence that *erg* channels play a role in spike frequency adaptation in another neuroblastoma-derived cell line, not dissimilar to the role of ganglionic M channels (Jones and Adams, 1987; Brown, 1988). In the present experiments, it appeared that inhibition of the fast (M) channels had more effect on the response of NG108–15 cells to a sustained current injection than did inhibition of the slow (merg) channels (Fig. 13). However, the relative contribution of these two currents to spike frequency adaptation may depend on the nature of the testing pulse protocol, because merg currents activate and deactivate more slowly than *KCNQ* currents, and hence accumulate during repetitive depolarization (Schonherr et al., 1999).

The transduction mechanism for M_1-mediated inhibition of *KCNQ2/3* and *merg1* is still unknown. Inhibition of I_{merg1a} and slow $I_{K(M,ng)}$ was accompanied by accelerated deactivation, which may indicate the involvement of protein kinase C (PKC); in *HERG* currents expressed in *Xenopus* oocytes, similar acceleration produced by thyrotropin-releasing hormone receptor activa-

tion was mediated by PKC (Barros et al., 1998). This would accord with an earlier proposal regarding the mechanism of inhibition of the M-like current in NG108–15 cells by bradykinin (Higashida and Brown, 1986). Although M_1 receptor activation in NG108–15 cells produces a strong elevation in intracellular $[Ca^{2+}]$ (Robbins et al., 1993), it is unlikely that Ca^{2+} could be a messenger for muscarinic inhibition of slow $I_{K(M,ng)}$ or I_{merg1a} because, in CHO cells, the Ca^{2+} ionophore ionomycin (5 μM) produced an insignificant reduction in I_{merg1a} (to 89.4 ± 9.7% of control; $n = 3$). As a control for the effectiveness of ionomycin in these cells, it caused a complete block of Kv1.2 channels expressed in CHO cells when recorded in perforated-patch or cell-attached configurations; direct application of 500 nM Ca^{2+} blocked Kv1.2 channels when recorded in the inside-out configuration (A. A. Selyanko and J. K. Hadley, unpublished observations).

Do products of *erg* genes contribute to M-like currents in other neurons? Transcripts for merg1 (London et al., 1997), and for the rat homologs erg1 and erg3 (Shi et al., 1997; Wymore et al., 1997) are present in mammalian brain. Furthermore, both expressed merg1a currents and the slow, presumed-merg1a component of the M-like current in NG108–15 cells were inhibited by stimulating M_1 muscarinic receptors, so they could contribute to muscarinic-inhibitable M-like currents previously recorded in central neurons. True, the presence of mRNA transcripts may not betoken the assembly of functional channels: thus, no appropriate *erg*-like component of membrane current could be recorded from mouse or rat sympathetic neurons, in spite of the presence of mRNAs (Shi et al., 1997; see also this paper), nor could we detect merg1 immunoreactivity. However, this may not be the case for other mammalian neurons. For example, the M-like current recorded from isolated rat cortical neurons has been reported to be an order of magnitude less sensitive to linopirdine than either the ganglionic or hippocampal cell current (Noda et al., 1998; cf. Aiken et al., 1995; Lamas et al., 1997; Schnee and Brown, 1998). Although other explanations are possible, our findings suggest that this might arise from a contribution by *erg* channels to the cortical neuron current. In view of the significance of M-like channels as potential targets for cognition-enhancing drugs (Zaczek and Saydoff, 1993), further information regarding the degree of heterogeneity in the molecular composition of the channels underlying M-like currents in different neurons would be helpful.

REFERENCES

Abogadie FC, Vallis Y, Buckley NJ, Caulfield MP (1997) Use of antisense-generating plasmids to probe the function of signal transduction proteins in primary neurons. In: Methods in molecular biology, Vol 83: Receptor signal transduction protocols (Challiss RAJ, ed), pp 217–225. Totowa, NJ: Humana.

Aiken SP, Lampe BJ, Murphy PA, Brown BS (1995) Reduction of spike frequency adaptation and blockade of M-current in rat CA1 pyramidal neurones by linopirdine (DuP 996), a neurotransmitter release enhancer. Br J Pharmacol 115:1163–1168.

Barros F, Gomez-Varela D, Viloria CG, Palomero T, Giraldez T, De-la-Pena P (1998) Modulation of human erg K^+ channel gating by activation of a G protein-coupled receptor and protein kinase C. J Physiol (Lond) 511:333–346.

Bernheim L, Mathie A, Hille B (1992) Characterization of muscarinic receptor subtypes inhibiting Ca^{2+} current and M current in rat sympathetic neurons. Proc Natl Acad Sci USA 89:9544–9548.

Bianchi L, Wible B, Arcangeli A, Taglialatela M, Morra F, Castaldo P, Crociani O, Rosati B, Faravelli L, Olivotto M, Wanke E (1998) Herg encodes a K^+ current highly conserved in tumours of different histogenesis: a selective advantage for cancer cells? Cancer Res 58: 815–822.

Biervert C, Schroeder BC, Kubisch C, Berkovic SF, Propping P, Jentsch T, Steinlein OK (1998) A potassium channel mutation in neonatal human epilepsy. Science 279:403–406.

Brown DA (1988) M-currents. In: Ion channels, Vol 1, (Narahashi T, ed), pp 55–94. New York: Plenum.

Brown DA, Adams PR (1980) Muscarinic suppression of a novel voltage-sensitive K^+ current in a vertebrate neurone. Nature 283:673–676.

Brown DA, Higashida H (1988a) Voltage- and calcium-activated potassium currents in mouse neuroblastoma x rat glioma hybrid cells. J Physiol (Lond) 397:149–165.

Brown DA, Higashida H (1988b) Inositol 1,4,5-trisphosphate and diacylglycerol mimic bradykinin effects on mouse neuroblastoma x rat glioma hybrid cells. J Physiol (Lond) 397:185–207.

Brown DA, Selyanko AA (1985) Two components of muscarine-sensitive membrane current in rat sympathetic neurones. J Physiol (Lond) 358:335–363.

Busch AE, Eigenburger B, Jurkiewicz NK, Salata JJ, Pica H, Suessbrich H, Lang F (1998) Blockade of HERG channels by the class III antiarrhythmic azimilide: mode of action. Br J Pharmacol 123:23–30.

Charlier C, Singh NA, Ryan SG, Lewis TB, Reus BE, Leach RJ, Leppert M (1998) A pore mutation in a novel KQT-like potassium channel gene in an idiopathic epilepsy family. Nat Genet 18:53–55.

Chiesa N, Rosati B, Arcangeli A, Olivotto M, Wanke E (1997) A novel role for HERG K^+ channels: spike-frequency adaptation. J Physiol (Lond) 501:313–318.

Constanti A, Brown DA (1981) M-Currents in voltage-clamped mammalian sympathetic neurones. Neurosci Lett 24:289–294.

Curran ME, Splawski I, Timothy KW, Vincent GM, Green ED, Keating MT (1995) A molecular basis for cardiac arrhythmia: *HERG* mutations cause long QT syndrome. Cell 80:795–804.

Faravelli L, Arcangeli A, Olivotto M, Wanke E (1996) A HERG-like K^+ channel in rat F-11 DRG cell line: pharmacological identification and biophysical characterization. J Physiol (Lond) 496:13–23.

Fukuda K, Higashida H, Kubo T, Maeda A, Akiba I, Bujo H, Mishina M, Numa S (1988) Selective coupling with K^+ currents of muscarinic acetylcholine receptor subtypes in NG108–15 cells. Nature 335:355–358.

Hamilton SE, Loose MD, Qi M, Levey AI, Hille B, McKnight GS, Idzerda RL, Nathanson NM (1997) Disruption of the m1 receptor gene ablates muscarinic receptor-dependent M current regulation and seizure activity in mice. Proc Natl Acad Sci USA 94:13311–13316.

Higashida H, Brown DA (1986) Two polyphosphatidylinositide metabolites control two K^+ currents in a neuronal cell. Nature 323:333–335.

Hu Q, Shi YL (1997) Characterization of an inward-rectifying potassium current in NG108–15 neuroblastoma x glioma cells. Pflügers Arch 433:617–625.

Jones SW, Adams PR (1987) The M-current and other potassium currents of vertebrate neurons. In: Neuromodulation (Kaczmarek LK, Levitan IB, eds), pp159–186. New York: Oxford UP.

Lamas JA, Selyanko AA, Brown DA (1997) Effects of a cognition-enhancer, linopirdine (DuP 996), on M-type potassium currents ($I_{K(M)}$) and some other voltage- and ligand-gated membrane currents in rat sympathetic neurons. Eur J Neurosci 9:605–616.

Lees-Miller JP, Kondo C, Wang L, Duff HJ (1997) Electrophysiological characterization of an alternatively processed ERG K^+ channel in mouse and human hearts. Circ Res 81:719–726.

London B, Trudeau MC, Newton KP, Beyer AK, Copeland NG, Gilbert DJ, Jenkins NA, Satler CA, Robertson GA (1997) Two isoforms of the mouse *ether-a-go-go*-related gene coassemble to form channels with properties similar to the rapidly activating component of the cardiac delayed rectifier K^+ current. Circ Res 81:870–878.

Marrion NV (1997) Control of M-current. Annu Rev Physiol 59:483–504.

Marrion NV, Smart TG, Marsh SJ, Brown DA (1989) Muscarinic suppression of the M-current in the rat sympathetic ganglion is mediated by receptors of the M_1-subtype. Br J Pharmacol 98:557–573.

Marsh SJ, Hubbard A, Brown DA (1990) Some actions of 9-amino-1,2,3,4-tetrahydroacridine (THA) on cholinergic transmission and

membrane currents in rat sympathetic ganglia. Eur J Neurosci 2:1127–1134.

Morielli AD, Peralta EG (1995) Suppression of a potassium channel by G-protein coupled receptors. Life Sci 56:1035.

Mullaney I, Dodd MW, Buckley N, Milligan G (1993) Agonist activation of transfected human M1 muscarinic acetylcholine receptors in CHO cells results in down-regulation of both the receptor and the α-subunit of the G-protein G_q. Biochem J 289:125–131.

Noda M, Obana M, Akaike N (1998) Inhibition of M-type K^+ current by linopirdine, a neurotransmitter-release enhancer, in NG108–15 neuronal cells and rat cerebral neurons in culture. Brain Res 794:274–280.

Owen DG, Marsh SJ, Brown DA (1990) M-current noise and putative M-channels in cultured rat sympathetic ganglion cells. J Physiol (Lond) 431:269–290.

Rae J, Cooper K, Gates P, Watsky M (1991) Low access resistance perforated patch recordings using amphotericin B. J Neurosci Methods 37:15–26.

Robbins JA, Caulfield MP, Higashida H, Brown DA (1991) Genotypic m3-muscarinic receptors preferentially inhibit M-currents in DNA-transfected NG108–15 neuroblastoma x glioma hybrid cells. Eur J Neurosci 3:820–824.

Robbins J, Trouslard J, Marsh SJ, Brown DA (1992) Kinetic and pharmacological properties of the M-current in rodent neuroblastoma x glioma hybrid cells. J Physiol (Lond) 451:159–185.

Robbins J, Marsh SJ, Brown DA (1993) On the mechanism of M-current inhibition by muscarinic m1 receptors in DNA-transfected rodent neuroblastoma x glioma cells. J Physiol (Lond) 469:153–178.

Sanguinetti MC, Curran ME, Spector PS, Keating MT (1996) Spectrum of *HERG* K^+ channel dysfunction in an inherited cardiac arrhythmia. Proc Natl Acad Sci USA 93:2208–2212.

Schafer S, Behe P, Meves H (1991) Inhibition of the M current in NG 108–15 neuroblastoma x glioma hybrid cells. Pflügers Arch 418:581–591.

Schnee ME, Brown BS (1998) Selectivity of linopirdine (DuP 996), a neurotransmitter release enhancer, in blocking voltage-dependent and calcium-activated potassium currents in hippocampal neurons. J Pharmacol Exp Ther 286:709–717.

Schonherr R, Rosati B, Hehl S, Rao VG, Arcangeli A, Olivotto M, Heinemann SH, Wanke E (1999) Functional role of the slow activation property of ERG K^+ channels. Eur J Neurosci 11:753–760.

Schroeder BC, Kubisch C, Stein V, Jentsch TJ (1998) Moderate loss of function of cyclic-AMP-modulated *KCNQ2/KCNQ3* K^+ channels causes epilepsy. Nature 396:687–690.

Selyanko AA, Robbins J, Brown DA (1995) Putative M-type potassium channels in neuroblastoma-glioma hybrid cells: inhibition by muscarine and bradykinin. Receptors Channels 3:147–159.

Singh NA, Charlier C, Stauffer D, DuPont BR, Leach RJ, Melis R, Ronen GM, Bjerre I, Quattlebaum T, Murphy JV, McHarg ML, Gagnon D, Rosales T, Peiffer A, Anderson VE, Leppert M (1998) A novel potassium channel gene, *KCNQ2*, is mutated in an inherited epilepsy of newborns. Nat Genet 18:25–29.

Shi W, Wymore RS, Wang HS, Pan Z, Cohen IS, McKinnon D, Dixon JE (1997) Identification of two nervous system-specific members of the *erg* potassium channel gene family. J Neurosci 17:9423–9432.

Spinelli W, Moubarak IF, Parsons RW, Colatsky TJ (1993) Cellular electrophysiology of WAY-123,398, a new class III antiarrhythmic agent: specificity of I_K block and lack of reverse use dependence in cat ventricular myocytes. Cardiovasc Res 27:1580–1591.

Titus SA, Warmke JW, Ganetzky B (1997) The *Drosophila erg* K^+ channel polypeptide is encoded by the seizure locus. J Neurosci 17:675–681.

Wang H-S, Pan Z, Brown BS, Wymore RS, Cohen IS, Dixon JE, McKinnon D (1998) KCNQ2 and KCNQ3 potassium channel subunits: molecular correlates of the M-channel. Science 282:1890–1893.

Wang XJ, Reynolds ER, Deak P, Hall, LM (1997) The *seizure* locus encodes the *Drosophila* homolog of the HERG potassium channel. J Neurosci 17:882–890.

Warmke JW, Ganetzky B (1994) A family of potassium channel genes related to *eag* in *Drosophila* and mammals. Proc Natl Acad Sci USA 91:3438–3442.

Wymore RS, Gintant GA, Wymore RT, Dixon JE, McKinnon D, Cohen IS (1997) Tissue and species distribution of mRNA for the I_{Kr}-like K^+ channel, *erg*. Circ Res 80:261–268.

Yang W-P, Levesque PC, Little WA, Condor ML, Shalaby FY, Blanar MA (1997) KvLQT1, a voltage-gated potassium channel responsible for human cardiac arrhythmias. Proc Natl Acad Sci USA 94:4017–4021.

Yang W-P, Levesque PC, Little WA, Conder ML, Ramakrishnan P, Neubauer MG, Blanar MA (1998) Functional expression of two KvLQT1-related potassium channels responsible for an inherited idiopathic epilepsy. J Biol Chem 273:19419–19423.

Yokoyama S, Imoto K, Kawamura T, Higashida H, Iwabe N, Miyata T, Numa, S (1989) Potassium channels from NG108–15 neuroblastoma-glioma hybrid cells. Primary structure and functional expression from cDNAs. FEBS Lett 259:37–42.

Zaczek R, Saydoff J (1993) Depolarization activated releasers of transmitters as therapeutics for dementia: preclinical characterization of linopirdine (DuP 996). Curr Opin Invest Drugs 2:1097–1104.